International Journal of Nanomedicine

Dovepress
open access to scientific and medical research

Open Access Full Text Article

ORIGINAL RESEARCH

Evaluating the biological risk of functionalized multiwalled carbon nanotubes and functionalized oxygen-doped multiwalled carbon nanotubes as possible toxic, carcinogenic, and embryotoxic agents

This article was published in the following Dove Press journal:
International Journal of Nanomedicine
19 October 2017
Number of times this article has been viewed

Luis A Lara-Martínez,[1] Felipe Massó,[2] Eduardo Palacios González,[3] Isabel García-Peláez,[4] Alejandra Contreras–Ramos,[5] Mahara Valverde,[6] Emilio Rojas,[6] Felipe Cervantes-Sodi,[7] Salomón Hernández-Gutiérrez[1]

[1]Department of Molecular Biology, School of Medicine, Universidad Panamericana, Mexico City, Mexico; [2]Department of Physiology, National Institute of Cardiology Ignacio Chavez, Mexico City, Mexico; [3]Department of Microscopy, Ultra High Resolution Electron Microscopy Laboratory, Instituto Mexicano del Petróleo, Mexico City, Mexico; [4]Department of Embryology, Medicine Faculty, Universidad Nacional Autonoma de Mexico, Mexico City, Mexico; [5]Department of Developmental Biology Research and Experimental Teratogenicity, Children's Hospital of Mexico, Federico Gomez, Mexico City, Mexico; [6]Department of Genomic Medicine, Institute of Biomedical Research, Universidad Nacional Autonoma de Mexico, Mexico City, Mexico; [7]Department of Physics and Mathematics, Nanoscience and Nanotechnology Laboratory, Universidad Iberoamericana, Mexico City, Mexico

Abstract: Carbon nanotubes (CNTs) have been a focus of attention due to their possible applications in medicine, by serving as scaffolds for cell growth and proliferation and improving mesenchymal cell transplantation and engraftment. The emphasis on the benefits of CNTs has been offset by the ample debate on the safety of nanotechnologies. In this study, we determine whether functionalized multiwalled CNTs (fMWCNTs) and functionalized oxygen-doped multiwalled CNTs (fCOxs) have toxic effects on rat mesenchymal stem cells (MSCs) in vitro by analyzing morphology and cell proliferation and, using in vivo models, whether they are able to transform MSCs in cancer cells or induce embryotoxicity. Our results demonstrate that there are statistically significant differences in cell proliferation and the cell cycle of MSCs in culture. We identified dramatic changes in cells that were treated with fMWCNTs. Our evaluation of the transformation to cancer cells and cytotoxicity process showed little effect. However, we found a severe embryotoxicity in chicken embryos that were treated with fMWCNTs, while fCOxs seem to exert cardioembryotoxicity and a discrete teratogenicity. Furthermore, it seems that the time of contact plays an important role during cell transformation and embryotoxicity. A single contact with fMWCNTs is not sufficient to transform cells in a short time; an exposure of fMWCNTs for 2 weeks led to cell transformation risk and cardioembryotoxicity effects.

Keywords: nanostructure, biocompatibility, scaffold, cell proliferation, cell cycle, carcinogenic

Introduction

Nowadays, nanoparticles play an important role as biomaterials for tissue regeneration.[1] Particularly, due to their physicochemical and structural characteristics, carbon nanotubes (CNTs)[2–4] have been highlighted as possible supports for cell growth. In fact, CNTs have already been used as scaffolds for cellular or tissue growth.[2,5–7] However, the essential impediments to their use in medicine continue to be uncertain about their biological safety and their influence on the human health. Although its cytotoxicity has been extensively studied, both in vivo and in vitro, as reviewed by Kayat et al,[8] there are some contradictory results that can be attributed to the use of materials with different degrees of purity and structural features,[9] as well as to the conditions adopted for the in vitro studies[10] and the types of cells tested in the assays.[11]

Several reports indicate that toxicity of CNTs seems to be similar to that of asbestos, as both materials share a fibrillar structure,[12] inducing mesotheliomas, ie, malignant tumors located in the pleural or abdominal cavities.[13,14] In addition, the preparation of

Correspondence: Salomón Hernández-Gutiérrez
Molecular Biology Laboratory, School of Medicine, Universidad Panamericana, Donatello 59 Colonia Insurgentes Mixcoac, 03290 Mexico City, Mexico
Tel +52 55 5482 1600 ext 5680
Fax +52 55 5482 1721
Email shernand@up.edu.mx

submit your manuscript | www.dovepress.com
Dovepress
http://dx.doi.org/10.2147/IJN.S144777

multiwalled CNTs (MWCNTs) has been recently classified as possibly carcinogenic to humans.[15]

In contrast, aspects of embryonic development have also been evaluated in other organisms. CNTs microinjected in the zebra fish model do not interfere with the embryonic development at 1-cell stage;[16–18] whereas, other studies suggest that at low concentrations CNTs induce fetal malformations in mice at 5.5 days postimplantation[19] but not in rats.[20] And in the chicken model, CNTs could have a very toxic effect on the normal development of the embryo.[21]

In spite of the widespread use of CNTs in biomedical applications, it is important to continue evaluating the innocuousness of these elements as toxic, carcinogenic, or embryotoxic agents among others for humans or other species. Today, these studies using MWCNTs must be designed according to their specific features, since postsynthetic treatments modify various properties that may have an impact on the safety and increase the risk for their use.[22] For example, in order to obtain biocompatible features from CNTs and because of their hydrophobic behavior, CNTs are commonly subjected to different functionalization processes. The most common of these involves an acid treatment, shortening the nanotube length and generating carboxylic groups at the walls of the CNTs, producing functionalized CNTs.[23–25]

The number of opportunities for cytological studies with CNTs is enormous; therefore, here, we narrow the object of study to mesenchymal stem cells (MSCs) and, in particular, stem cells derived from bone marrow (BM).

MSCs represent an attractive option in cellular therapy, for example, in the regeneration of endothelial and cardiac cells of damaged tissue as in myocardial ischemia.[26] However, the proliferative capacity of MSCs is highly dependent on their application methodology. For example, due to the lack of anchorage between damaged cardiac tissue and supplied cells, if the MSC suspensions are directly applied into the damaged area, the improvement of the surrounding damaged tissue produces little to null improvements.[27] Therefore, the production of adequate scaffolds for the proliferation and anchorage of MSCs is fundamental to engineer functional cardiac tissue constructs in vitro.[28,29] Some studies have gone further and focused on the development of CNTs in nanofiber scaffolds that simulate the architecture of the myocardium tissue repairing the affected cardiac areas.[30,31]

A significant advantage derived from working with primary cultures of MSCs is to ensure a clean and clear genetic background without the presence of genetic disorders such as those accumulated in traditional cell lines previously preestablished and characterized.[32] In addition, MSCs present a high sensitivity toward inducing changes in their multipotent differentiation patterns[33–35] and proliferation.[36] Therefore, MSCs are an excellent model to evaluate several biological parameters such as proliferation, apoptosis, anchorage, and cytotoxicity.[29] Although the safety of MSCs application has been emphasized in several reports,[37] their exposure to different carcinogens in functionalization process could initiate some types of cancer, but until now, the role of fCNTs as possible carcinogen in MSCs remains unknown.

Several applications of CNTs require different ways of chemical alterations in order to tune their physicochemical characteristics and their biological compatibility. Doping and functionalizing CNTs are the two most used ways to modify CNTs.[38] Doping consists of the substitution of one or more carbon atoms for an atom of a different element, involving covalent bonding. It is usually performed while the nanotube is being synthesized. Functionalization is another process where the as-grown CNTs are subjected to a series of chemical processes.[38]

In previous biological reports, oxygen-doped MWCNTs (COxs)[39,40] have been used due to the presence of carbonyl, hydroxyl, and oxygenated functional groups enhancing their chemical reactivity, in addition to their higher water solubility[25]

Prior to considering MWCNTs as biological scaffolding for grown MSCs in future cardiac protocols, in this study, we aim to evaluate the possible adverse effects on cells and cardiac tissues, using two kinds of CNTs, such as acid functionalized MWCNTs (fMWCNTs) and functionalized oxygen-doped multiwalled CNTs (fCOxs). The objective is to study the effect of fMWCNTs and fCOxs at different concentrations in two biological models with the following purposes: first, on rat MSCs focusing on their growth, proliferation, cell cycle, and possible cell transformation processes to cancer cell and, second, using an in vivo chicken model to study the cardioembryotoxicity.

Methods

Preparation of CNTs

Both types of nanotubes (MWCNTs and COxs) used in this study were synthesized by chemical vapor deposition (CVD) following procedures similar to those reported by other authors.[41,42] Mainly, a tubular furnace with a quartz tube reactor is heated under a 0.2 L/minute Ar flow. After reaching 850°C, microdroplets of two different solutions are supplied by a sprayer (Pyrosol; RBI, Meylan, France) by an Ar flow of 1.5 L/minute in order to obtain each kind of nanotube. For MWCNTs and COxs, the following solutions were prepared and used: ferrocene/toluene and ferrocene/toluene/ethanol at 3.5/96.5 and 3.5/94.5/2.0 wt% respectively, from

Sigma-Aldrich (St Louis, MO, USA). After 40 minutes of CVD reaction, the sprayer is turned off and, after extracting the quartz tube from the furnace, the as-obtained CNTs were carefully scratched from the central part of the quartz reactor, obtaining a black powder consisting of small flakes of CNT "forests", as shown in Figure 1A. After the synthesis, both types of nanotubes are chemically functionalized by an acid treatment.[43] A total of 10 mg of

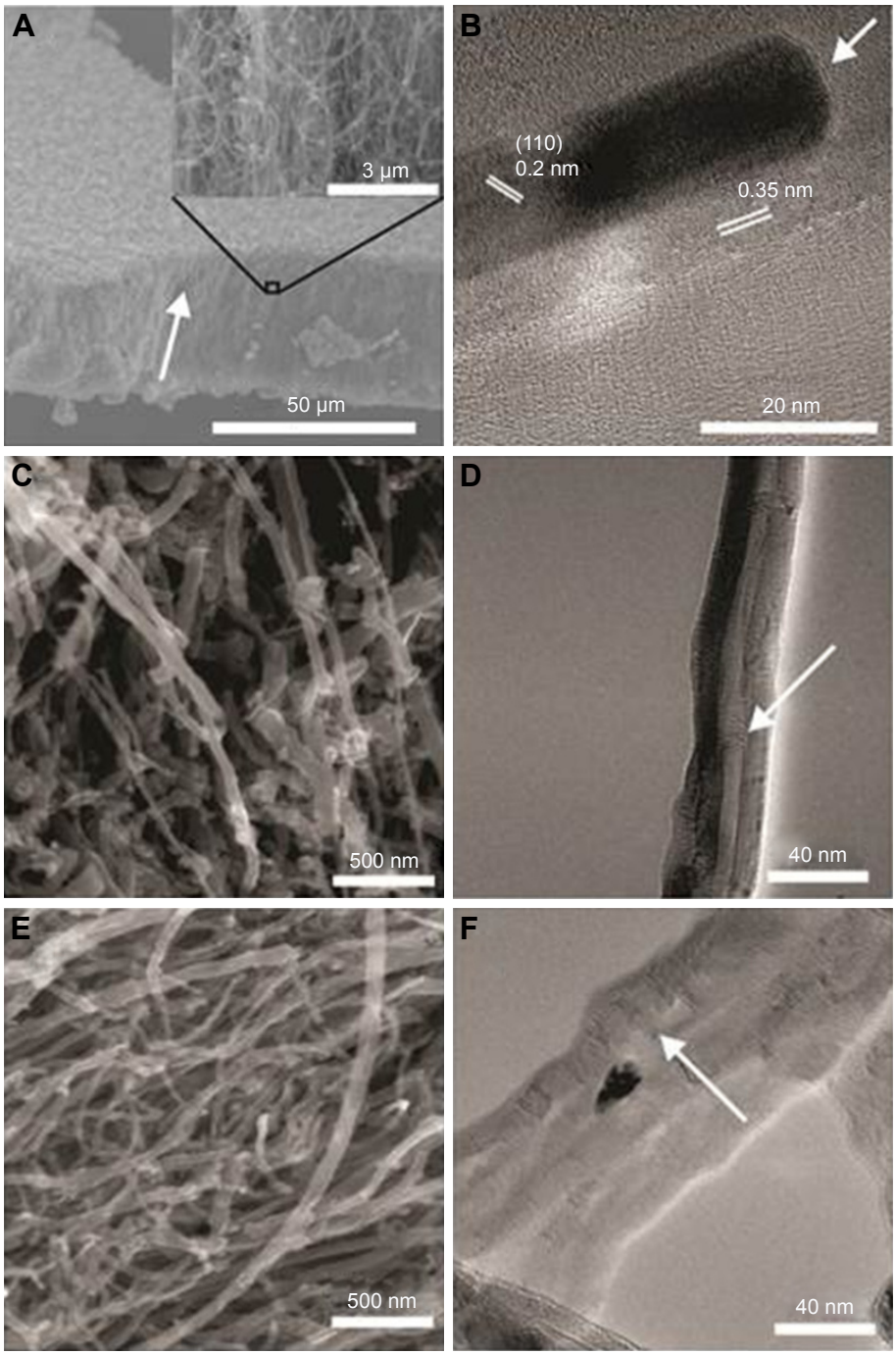

Figure 1 SEM and TEM micrographs of CNTs.
Notes: (**A**) Representative image of the startup material, ie, the as-grown "forest" of CNTs. The white arrow indicates the growth direction of the intertwined CNTs and their preferential vertical alignment, better appreciated in the top inset. (**B**) High-resolution TEM micrograph showing the crystallographic planes of both the nanotube and the Fe catalytic particle. The arrow indicates the formation of a bamboo-like structure. The estimated interplanar distances measured using ImageJ[53] are very close to the graphene–graphene interlayer for the MWCNTs and the interplanar distances for *bcc* Fe in the 110 crystallographic direction. SEM/TEM micrographs of functionalized fMWCNTs (**C**/**D**) and functionalized fCOxs (**E**/**F**). The overall morphologies and structure of the tubes are shown, indicating with arrows the typical bamboo-like formations. The main difference between MWCNTs and COxs appreciated by SEM and TEM is the higher diameter of MWCNTs and the slightly more disordered (more bamboo-like) formations in fCOxs.
Abbreviations: CNTs, carbon nanotubes; COxs, oxygen-doped MWCNTs; fCOxs, functionalized oxygen-doped multiwalled CNTs; fMWCNTs, functionalized MWCNTs; MWCNTs, multiwalled CNTs; SEM, scanning electron microscopy; TEM, transmission electron microscopy.

CNTs are ultrasonicated (Ultrasonic Processor CP750 at 750 W and 20 kHz; Cole-Palmer; Vernon Hills, IL, USA) for 4 hours in 500 mL of an acid solution of bidistilled water/H_2SO_4/HNO_3 at 92.5/5.5/2 vol% pure acids (Sigma-Aldrich). Then, the solution is filtered and washed with bidistilled water several times, obtaining usable fMWCNTs and fCOxs.

Finally, solutions of each kind of CNTs at 10 mg/mL are prepared using bidistilled water during 2 hours of ultrasonication (750 W and 20 kHz). Samples are set for scanning electron microscopy (SEM) and transmission electron microscopy (TEM) by dispersing in acetone for 15 minutes in a Branson 1510 Ultrasonic Cleaner (70 W and 42 KHz) (Danbury, CT, USA) and drop casting in the corresponding SEM holders and TEM grids.

Characterization of CNTs

Observation and analysis of the samples were performed using two SEM; a FEI Dual-Beam Nova-200 Nanolab, coupled with an X-ray Si (Li) ultrathin window energy dispersive spectrometer for low atomic number detection, and a Hitachi model SU3500. TEM micrographs were obtained in a Tecnai G2 F30 S-TWIN TEM microscope. Raman spectra were collected using a LabRAM HR 800 model (HORIBA Jobin Yvon ; Kyoto, Japan), using a laser line of 532 nm at a power of 43.4 mW and the exposure times of ~20 seconds. Thermogravimetric analysis (TGA) was performed using a Perkin Elmer TGA-7 (Waltham, MA, USA) with a temperature interval of 25°C–800°C heating at 5°C/minute under a dry air flux of 20 mL/minute.

Cell culture and analysis of cell viability

After three passes, 5×10^4 MSCs from rat's BM, previously isolated and cloned from a heterogeneous primary culture,[44] were grown in 24-well plates with α-minimum essential medium (Merck Millipore, Billerica, MA, USA) supplemented with 10% fetal bovine serum, 10,000 U penicillin, 10 mg of streptomycin, and 25 mg of amphotericin B per milliliter (Thermo Fisher Scientific, Waltham, MA, USA) at different CNT concentrations (10, 100, and 1,000 ng/mL) with their respective controls. Cytotoxicity and viability of MSCs were assessed with 0.2% Trypan blue staining T-6146 (Sigma-Aldrich). Briefly, media were discarded and cells were washed with 1× phosphate buffered saline (PBS) three times after adding precooled Trypsin I with 0.25% (w/v) diluted Gibco in 1× PBS and adding 0.2 mL in each well followed by incubation at 37°C for 5 minutes. Cells were pelleted gently at 1,600 rpm for 5 minutes, resuspended in complete DMEM with 10% FBS, and counted with 0.2% Trypan blue in a 1:1 ratio. The stained cells were excluded using an accomplished hemocytometer. Three independent trials each in triplicate at 0, 24, 48, and 72 hours and 7 days. The percentage of live cells was determined, and an analysis of variance was performed using Tukey's test using Prism 4.0 (GraphPad Software, Inc., La Jolla, CA, USA) to establish differences between populations.

Cell cycle analysis

Cells from each experimental condition were collected by centrifugation and were fixed and stained with propidium iodide staining solution (50 µg/mL) in the presence of 0.5 µg/mL of RNase A in the dark for 30 minutes following the methodology described elsewhere.[45] The stained cells were subsequently analyzed on a FACSCalibur flow cytometer (BD, Franklin Lakes, NJ, USA) using CellQuest acquisition software (Version 3.3; BD Immunocytometry Systems; Franklin Lakes, NJ, USA). Automated DNA content quantification was carried out with ModFit LT software (Verity Software House Inc., Topsham, ME, USA). The %G1 was defined as the area of the G1 model peak divided by the combined areas of the G1 and G2/M peaks. In each sample, 20,000 cells were sorted. The population doubling time was calculated accordingly,[46] for each condition of fCNTs' treatment and their respective control.

Spatial determination of nanotubes by light field and confocal microscopy

To reveal the presence of fCNTs, control and treated cells were grown on coverslips during 7 days, washed with PBS, and fixed with paraformaldehyde (PFA) at 4% for 24 hours at 4°C. The cells were stained for 2 minutes with toluidine blue (1%) and dissolved in aqueous solution of borax 1%. The dye was removed and washed with PBS and observed under a microscope Axioplant 2 Zeiss (Carl Zeiss Meditec AG, Jena, Germany).

In contrast, the fCNTs in suspension and their presence inside the cells were revealed by photoluminescence spectra using a laser beam at 488 nm and an emission filter LB 505–530 nm;[47] a nuclear staining was performed using DRAQ7 (BioStatus, Leicestershire, UK) and seen at filter LP 633 nm. Images were captured using a confocal microscope (Carl Zeiss Meditec AG; Oberkochen, Germany) and Zen 2009 software. This research was approved by Bioethics Committee of Faculty of Health Sciences of the Panamerican University.

Anchorage-independent cell growth in agar and tumorigenicity assays

To determine anchorage-independent cell growth, 1×10^2 MSCs treated and not treated with fCNTs at different

concentrations (10, 100, and 1,000 ng/mL) were seeded in 60 mm culture dishes that were previously treated with different CNT concentrations in complete medium containing 1.3% methyl cellulose (Sigma-Aldrich) over a layer of 1.2% of semisoft agar (Difco, Detroit, MI, USA) as previously described.[48] The resulting colonies were counted and photographed 2 weeks later; the murine tumorigenic B16F-10 (purchased from ATCC CRL-6475) cell line was used as a positive control. The results show the mean and SD of three independent experiments.

Nude mice assay

Nude mice BALB/C-nu/nu is a well-known model that allows evaluating the tumorigenic potential of transformed cells inoculated in them. As a result from a mutation in the Foxn1, the mice strain is immunodeficient and completely lacks a thymus;[49] this condition leads to many defects in the immune system and, therefore, must be maintained isolated under special conditions.

The tumorigenicity was determined in 8-week-old BALB/C-nu/nu male specific pathogen-free mice by subcutaneous injection of 1×10^6 MSCs treated and not treated with fCNTs at the same concentrations mentioned earlier or B16F-10 cells as positive control, both suspended in 0.2 mL of PBS. A total of 30 mice were tested for each group of fCNTs. The mice were provided by National Institute of Medical Sciences (INCMNSZ Ciudad de Mexico, Mexico), kept in microisolation boxes, fed, filtered, and sterilized water ad libitum. The injection sites were observed regularly for the development and progression of tumors. Size tumor volume was determined using the formula $L \times W^2/2$, as reported by Bullard et al.[50] All animals used in this study were maintained under standards established by the guidelines for animal care and use of NOM-039 NORMA Official Mexicana NOM-062-ZOO-1999 and previously approved by the Institutional Animal Care and Use Committee of the Faculty of Health Sciences at the Panamerican University.

Embryotoxicity assays

To detect the toxicity of fCNTs in vivo, 85 fertilized chicken embryos were incubated per group at 37.5°C and 86%–87% humidity in a forced-draft incubator. The embryos were injected directly in pericardio with a G1 capillary micropipette (Narishige Co., Tokyo, Japan) at developmental stage 22 as defined by Hamburger and Hamilton (HH).[51] To access the embryo, a small window was opened in the shell and the membranes surrounding the embryo were removed. The embryo was injected with 1.5 µL of fMWCNTs and fCOxs at 100 and 1,000 ng/mL in PBS and 1.5 µL PBS in controls; a sham group was also evaluated. The window was sealed, and embryonic development was allowed to continue for a week, at the end of which the embryos were sacrificed and analyzed for morphological alterations. For confocal assay studies, hearts were fixed in 10% neutral buffered formalin, frozen, and sectioned in sagittal plan. Tissue slices of 5 µm thickness were washed with 1× PBS and fixed with 4% (w/v) PFA (Sigma-Aldrich) to be later permeabilized with 0.1% Triton X-100 and finally blocked with 1% horse serum and 1% BSA in TBS. Samples were incubated at 4°C overnight with anti-SMA (1:200). In the following day, slices were washed three times with 1× PBS and incubated at room temperature during 1 hour using Rhodamine (Jackson ImmunoResearch Laboratories, Inc., West Grove, PA, USA) secondary antibodies (1-600). After three additional washes with 1× PBS, a nuclear staining was performed using DRAQ7 and the samples were visualized and photographed under a laser scanning confocal microscope (LSM 410; Axiovert 100, Zeiss 40× plan-Neofluor WD 13.5 mm; Carl Zeiss Meditec AG).

Statistics

Three independent experiments were performed with three replicates per group for each biological experimental treatment to be done. Data are expressed as a mean ± standard deviation of the experiments. Statistical analysis was performed by analysis of variance with Tukey's test to determine significant differences. Values are shown as mean ± standard deviation; significance was inferred at $^{**}P<0.01$ and $^{*}P<0.05$.

Results

Properties of CNTs

The as-grown MWNTs and COxs present a preferential alignment perpendicular to the substrate area, forming what is commonly known as "nanotube forests". Figure 1A presents low magnification SEM images of representative grown CNTs with an inset at higher magnification. The preferential growth direction is shown by the white arrow. Pristine CNTs present lengths of up to hundreds of micrometers, with huge length-to-diameter aspect ratios.

As mentioned earlier, both types of nanotubes used here are of the multiwall form, meaning that they are conformed by several coaxial layers of tubular graphene sheets, as shown in the representative TEM micrograph in Figure 1B. This high-resolution micrograph shows a close up of a MCWNT with 20 graphene layers in contact with the Fe catalytic (darker region). The interlayer distance between graphitic layers is close to the typical interlayer distance in graphite (ie, 0.36 nm), whereas the interlayer distance of ~0.203 nm in the catalytic particle

corresponds to the (110) planes of iron *bcc*. It is very common that catalytic particles remain encapsulated inside the nanotubes during growth. Note that, in the upper part of the Fe particle, a thin layer of carbon is formed, which is also usually found in MWCNTs and COxs, called bamboo-like structures (indicated by the small arrow and by the arrows in Figure 1D and F). Among CNTs, the purity and crystallinity of the graphene layer is decreasing from single-walled CNTs[43] to MWCNTs. Defects in nanotubes are any alteration of the graphitic lattice, including exohedral, endohedral, and in-plane doping; they are common in the CNTs synthetized by the present method[38] and have been well characterized elsewhere.[39–41,52] An atomistic difference between MWNTs and COxs is difficult to appreciate by SEM and TEM, since, as discussed by Botello-Méndez et al,[39] Shabestari et al,[40] and González et al,[52] the meaning of oxygen doping is the formation of different atomic alterations in the graphene layers as carbon–oxygen bonds (eg, by the use of X-ray photoelectron spectroscopy)[52] present the percentage of carbon atoms in graphitic or aliphatic bonds or as part of functional groups such as alcohol, lactones, and carboxyl. This functional group makes COx slightly more reactive than nondoped or MWCNTs. However, pristine nanotubes, both MWCNTs and COx, are highly hydrophobic without a further chemical functionalization.

Morphology differences between fMWCNTs and fCOx are minor. In cases, as mentioned earlier, the nanotubes are of multiwall type and TEM micrographs show bamboo-like structures (indicated by arrows in Figure 1D and F). High aspect ratio is presented prior to functionalization; however, one of the effects of the functionalization process is the breaking of nanotubes after which nanotubes are cut and lengths are difficult to estimate (Figure 1C and D).

Measurements of Raman spectra and TGA of functionalized nanotubes are shown in Figure 2. The information obtained from both spectra is critical to characterize the purity and reactivity of the nanotubes. Typical D and G bands are present in spectra of both fMWCNTs and fCOx at ~1,344 and 1,580/cm, respectively (Figure 2A).

The effect of functionalization is clear; there is a relatively low degree of graphitization (order), with a D/G Raman intensity ratio (disorder) with values 0.44 for fMWCNTs and 0.55 for fCOxs (very similar to the D/G value reported previously).[52] In this study, the disorder is necessary to make the nanotubes hydrophilic and dissolve them in water solutions. Furthermore, TGA was performed in both samples. The analyses show decomposition temperatures of fMWCNTs and fCOxs of 580 and 560°C, respectively (Figure 2B). Oxygen doping induces higher surface reactivity of CNTs. The oxidation reduction temperature is caused by the introduction of additional carboxylic and other functional groups, prior to the functionalization, on the graphitic surfaces of CNTs. As a summary of the characteristics of functionalized CNTs, Table 1 includes the main structural and physicochemical characteristics of the fMWCNTs and fCOxs used throughout this study, which are in good agreement with the already mentioned literature. The estimated interplanar distances were measured using ImageJ.[53]

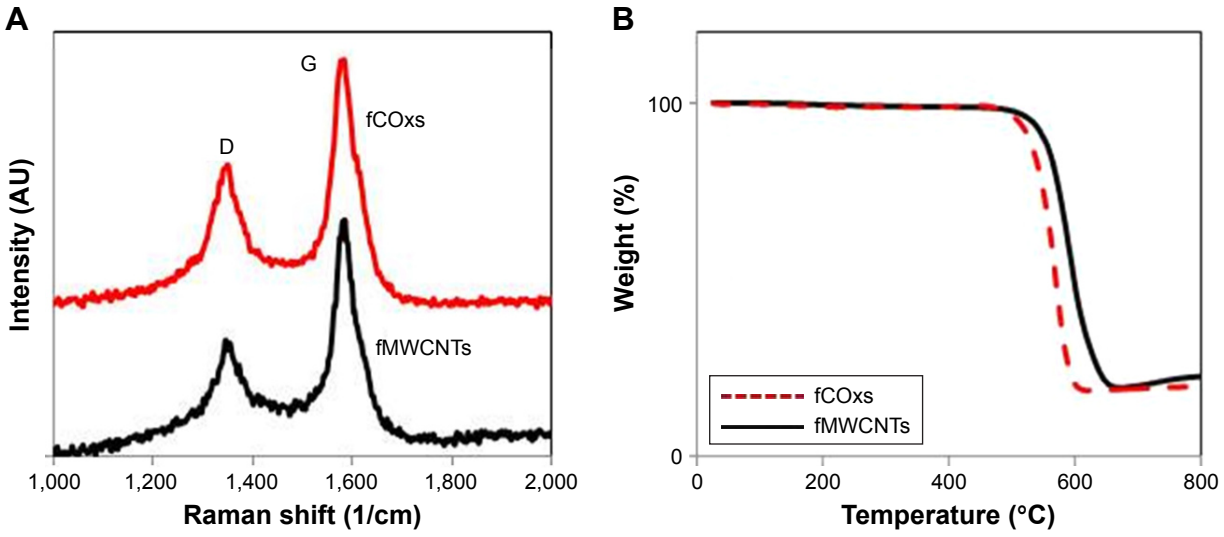

Figure 2 Raman spectra and TGA of fMWCNTs and fCOxs.
Notes: (**A**) Raman spectra show a high degree of disorder in both fMWCNTs and fCOxs (high D/G ratio). The functionalization through the acid treatment introduces functional groups and disorder in the nanotube walls, increasing the D/G ratio. (**B**) TGA of fMWCNTs and fCOxs in dry air; fCOxs decomposed at lower temperature, exhibiting a faster oxidation rate than fMWCNTs. The materials reveal a decomposition temperature of 580°C for fMWCNTs and 560°C for fCOxs.
Abbreviations: fCOxs, functionalized oxygen-doped multiwalled carbon nanotubes; fMWCNTs, functionalized multiwalled carbon nanotubes; TGA, thermogravimetric analysis.

Table 1 Typical structural parameters of nanotubes

Structural parameter	fMWCNTs	fCOxs
Length prior to functionalization (μm)	600±100	500±100
Diameter (nm)	66±25	26±10
D/G intensity ratio	0.44	0.55
T decomposition (°C)	580	560
Atom% C[a]	99.5	94.4
Atom% Fe[a]	0.5	1.7
Atom% O[a]	–	3.9

Notes: [a]Atomic percentage of elements from EDS. Data presented as mean ± standard deviation of the parameter.
Abbreviations: EDS, energy dispersive spectrometer; fCOxs, functionalized oxygen-doped multiwalled carbon nanotubes; fMWCNTs, functionalized multiwalled carbon nanotubes.

Effect of fMWCNTs and fCOxs on cell proliferation

The results of cell proliferation of MSCs isolated from rat's BM under different concentrations of fMWCNTs and fCOxs (10, 100, and 1,000 ng/mL) are presented in Figure 3. In MSCs, no group differences were found at 24 hours; however, cell cultures with fMWCNTs present significant increment after 48 and 72 hours of culture, while fCOxs present significant increment only after 72 hours. The same increase trend is observed for the 1-week culture (Figure 4), where the three concentrations present an approximately twofold proliferation increase with respect to control, and almost no differences among different concentrations.

Effect of fMWCNTs and fCOxs on cell cycle

Cell cycle, evaluated by flow cytometry during exponential growth phase, evaluates alterations in treated cells as shown in Figure 5. The cells stimulated by fMWCNTs pass faster through the S and G2/M phases, shortening the time for each cycle in comparison with fCOx or control cells. To confirm cell cycle alterations, we used an important parameter for the description of dynamics of cellular growth, called the cell doubling time, indicating the proliferation decontrol in treated cells. Table 2 shows the data obtained for the different groups with and without fMWCNTs or fCOxs. The doubling times for treated cell are shorter by ~25% in both cases, implicating a faster growth for fCNT-treated cultures with almost a 50% increment in the number of generations. Differences between fMWCNTs and fCOx cultures are ~5%–10%.

Cellular morphological alterations

Exposing cells to different concentrations of fCNTs during a week time generates evident morphological alterations only in the cells cultured with fMWCNTs at 100 and 1,000 ng/mL.

The observation of the negative controls and the fCOx-treated group indicates an absence of morphological changes. Morphological analysis of cells treated with fMWCNTs showed diverse changes (Figure 6B) mainly in the formation of ovoid cell clusters with giant nuclei and the presence of multiple nucleoli, as well as the appearance of several cells in mitosis (arrows). No morphological changes were detected in cells treated with fCOx (Figure 6C) or in control (Figure 6A). The presence of fCNTs in culture was detected using a blue staining to contrast the cells, which shows the CNTs in black only in treated cells with fMWCNTs (Figure 6E) or fCOxs (Figure 6F) but not in controls (Figure 6A and D). Confocal microscopy was also revealed its presence as inductors responsible for morphological alterations. fMWCNTs were colocalized with nucleus inside cytoplasm (Figure 6H) but not in fCOx-treated cells (Figure 6I) or control (Figure 6G).

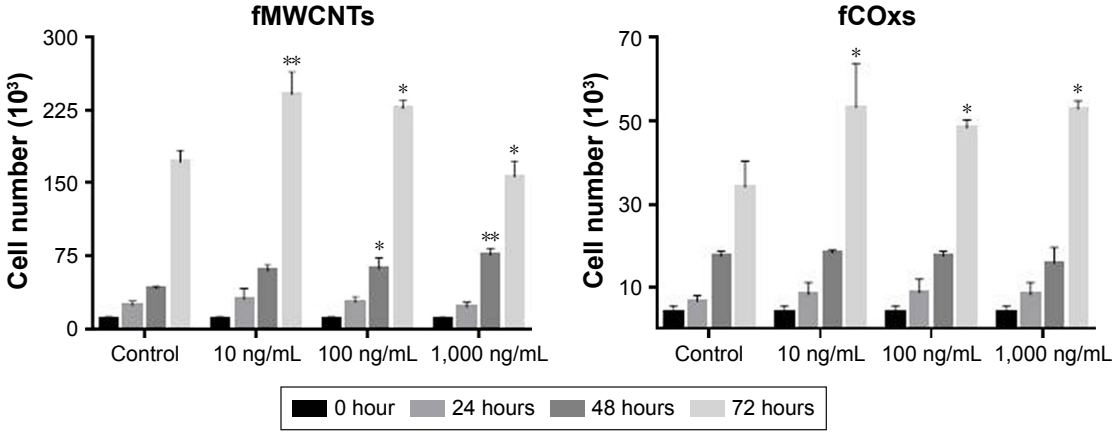

Figure 3 Proliferation effects on MSCs versus incubation time at different fMWCNTs and fCOx concentrations.
Notes: The percentage of viable cells was determined after each treatment as is indicated and compared with their respective control. Analysis of variance determined significant differences between control and treated groups for the incubation times over 24 hours. Values are shown as mean ± standard deviation (**$P<0.01$ and *$P<0.05$).
Abbreviations: fCOxs, functionalized oxygen-doped multiwalled carbon nanotubes; fMWCNTs, functionalized multiwalled carbon nanotubes; MSCs, mesenchymal stem cells.

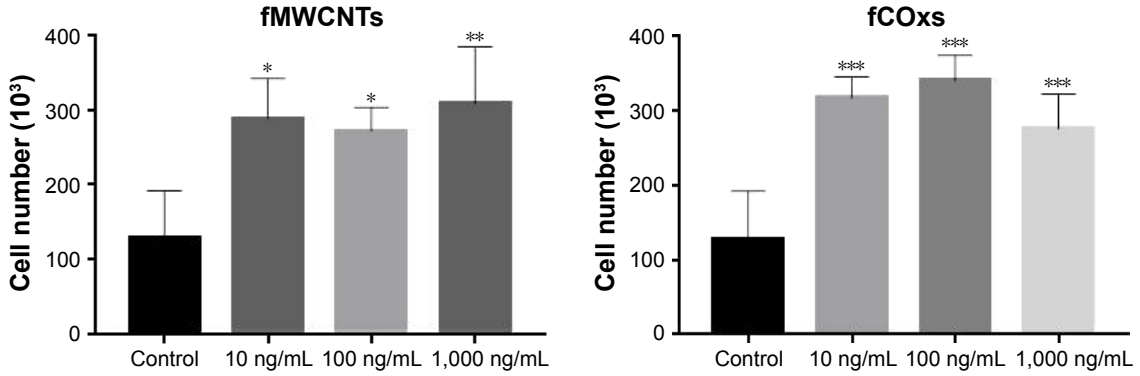

Figure 4 Chronic effect on proliferation of rat MSCs treated with fMWCNTs and fCOxs.
Notes: Cells were cultured and treated with each fCNTs solution for a 7-day time period at different concentrations; afterward, cell counts and the analysis of variance determined significant differences between control and treated groups, with higher than twofold increases for all concentrations. Values are shown as mean ± standard deviation (***$P<0.001$, **$P<0.01$, and *$P<0.05$).
Abbreviations: fCOxs, functionalized oxygen-doped multiwalled carbon nanotubes; fMWCNTs, functionalized multiwalled carbon nanotubes; MSCs, mesenchymal stem cells.

Otherwise, the cytoplasm of the control cells is retracted, unlike the treated cells, which have a more extensive area such that their initial elongated morphology is lost.

The evident cellular changes in cell cycle and morphology, both induced clearly only by fMWCNTs, led us to consider the association of these nanotubes with a possible cell transformation potential. In order to evaluate the potential carcinogenicity of fCNTs, their capacity to transform a normal cell (MSCs) to a tumor cell, we perform two assays, first by forming colony in agar growth and, second, by evaluating their tumorigenic capacity in nude mice cells, as explained later.

Cellular growth with anchorage independence and tumorigenicity assays

This assay is a technique widely used to evaluate cell transformation in vitro by soft agar assays. Although there is evidence that CNTs can act as cocarcinogen, it is not clear whether they could generate malignant cells by themselves. Thus, we decided to evaluate the potential carcinogenic of fMWCNTs or fCOxs on MSCs seeded in soft agar. MSCs were treated and untreated during 2 weeks at different concentrations (10, 100, and 1,000 ng/mL) with fMWCNTs or fCOxs; B16F-10 cells were used as positive control. After 3 weeks of growth, the colonies formed were counted. The percentage of colonies' growth by treated cells and their respective controls is shown in Table 3. Any group of MSCs treated with fCNTs presents a significant difference when compared with nontreated group, with the highest difference of 8% corresponding to the 100 ng/mL concentration of fMWCNTs. The obtained growth of the colonies' percentages is the expected for positive control (B16F-10 cells).

Tumorigenicity in vivo

The tumorigenic potential of MSCs cultured with fCNTs during 2 weeks was evaluated in a strain of immunosuppressed nude mice. After cultured, cells were subcutaneously injected into the mice flanks. The injection sites were observed regularly for the development and progression of

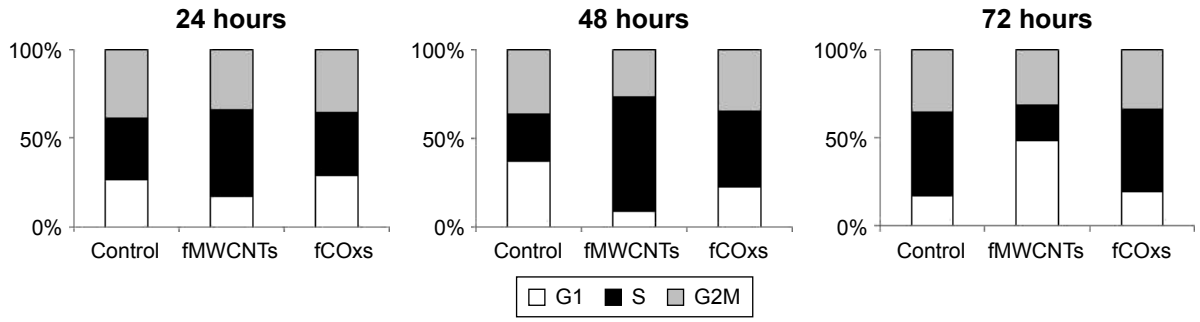

Figure 5 Cell cycle phase analysis.
Notes: Cell cycle of MSCs was altered by the presence of fCNTs. The cells were seeded with fMWCNTs or fCOxs to a final concentration of 100 ng/mL and were marked with propidium iodide, and the cell cycle assay by flow cytometry was performed. Control cells were treated with vehicle. Graphical summary of each point shows treated cells passing faster through the S and G2/M phases than control cells.
Abbreviations: fCOxs, functionalized oxygen-doped multiwalled carbon nanotubes; fMWCNTs, functionalized multiwalled carbon nanotubes; MSCs, mesenchymal stem cells.

Table 2 Cell doubling time

	Control	fMWCNTs	fCOxs
Doubling time (hours)	37.96	27.48	29.09
Number of generations	4.19	6.11	5.79

Notes: The effect of CNTs on MSCs shows a reduction in the cell doubling time calculated for each treated group. The number of generations was also included. The number of generations was evaluated after 7 days of treatment.
Abbreviations: CNTs, carbon nanotubes; fCOxs, functionalized oxygen-doped multiwalled CNTs; fMWCNTs, functionalized multiwalled CNTs; MSCs, mesenchymal stem cells.

tumors. After 30 days, postinjection mice were sacrificed. Interestingly, any group of the injected mice produced tumors, the only tumors were found, as expected, in those mice injected with B16F-10 cells (Table 3).

Embryotoxicity tests

Finally, we evaluated whether the same concentrations of fCNTs that cause morphological changes in vitro (100 and 1,000 ng/mL) can compromise embryonic development when the solutions are injected into the chick heart. Figure 7 shows the mortality rate induced by fMWCNTs and fCOxs and their respective control, revealing that fMWCNTs produce a severe embryotoxicity in which both concentrations prevented cardiac-embryonic development, with the majority dying at stage 28 HH. Cardiac alterations induced by fMWCNTs were mainly characterized by the lack of spatial rotation of the outflow tract, generating bilateralism with the inflow tract and interventricular communications;

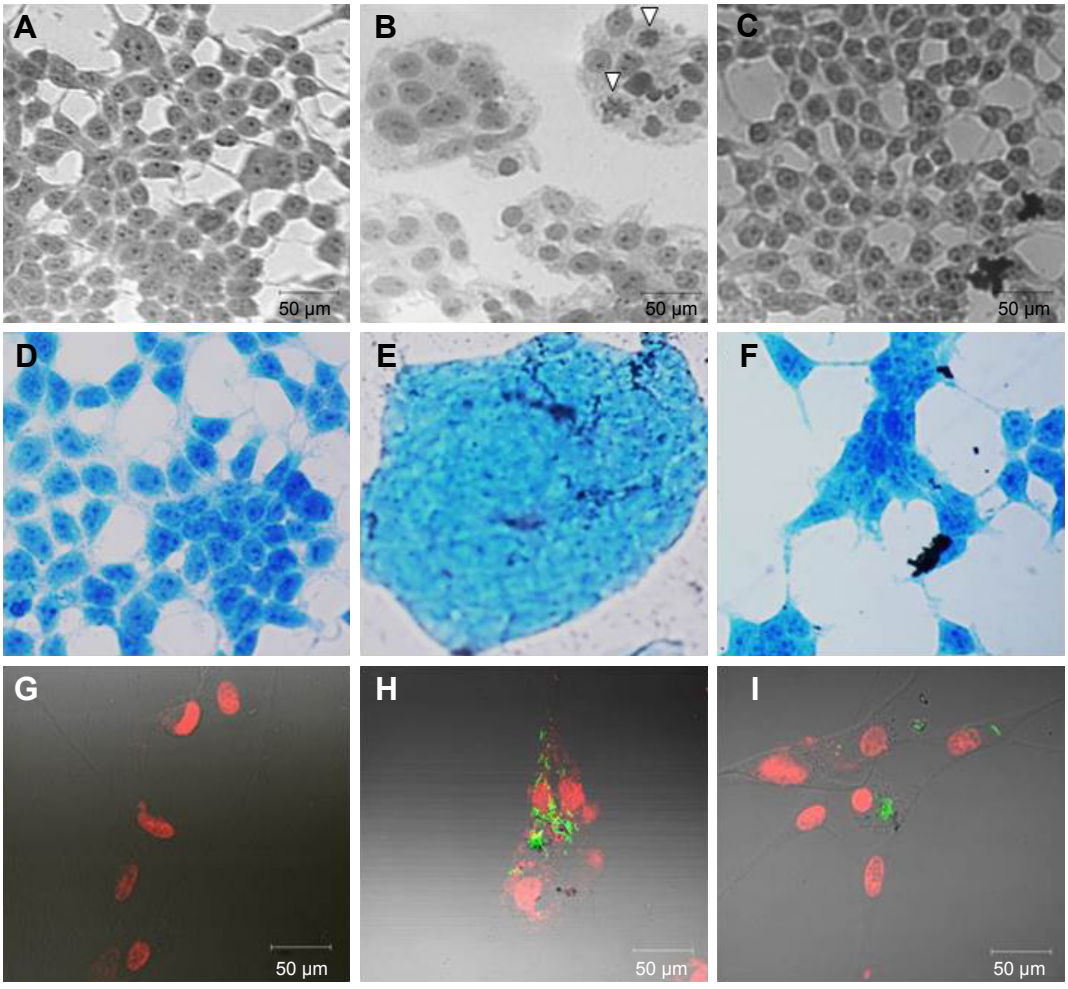

Figure 6 Morphological and confocal analyses.
Notes: The cell morphology of MSCs was altered by fMWCNTs. (**A**) Typical control image of nontreated cells. (**B**) Cellular morphology after 7 days treatment with 100 or 1,000 ng/mL of fMWCNTs; cells lost their polygonal shape, increased the cytoplasm area, and appeared with numerous nucleoli; furthermore, some cells in mitosis are observed (white arrows). (**C**) The morphology of cells with fCOx treatment is unaltered. For the detection of CNTs associated with morphological changes, a spatial determination of fCNTs by light visible and confocal microscopy was performed. The cells were stained with toluidine blue for a better contrast under visible light: (**D**) untreated cells, (**E**) presence of morphological changes induced by cytoplasmic incorporation of fMWCNTs into the MSCs, and unlike those (**F**) cells treated with fCOxs that do not present the incorporation of nanotubes into the cells; nanotubes remain outside of the cells. The presence of CNTs was also revealed using confocal microscopy for each group. (**G**) Control cells and (**H**) nuclear colocalization fCNTs with apparent damage induced by cytoplasmic incorporation of fMWCNTs. (**I**) fCOxs remain outside of the cells without cell morphological affectation.
Abbreviations: CNTs, carbon nanotubes; fCOxs, functionalized oxygen-doped multiwalled CNTs; fMWCNTs, functionalized multiwalled CNTs; MSCs, mesenchymal stem cells.

Table 3 Effect of fMWCNTs and fCOxs on colony formation and tumorigenicity of MSCs

Treatment	Colony formation (%)	Tumorigenicity	Tumor size, cm^3
Positive control	62±4.4*	10/10	2.19±0.61
MSC control	2.66±1.2	0/10	NT
MSC + fMWCNT 10 ng/mL	3.44±1.2	0/10	NT
MSC + fMWCNT, 100 ng/mL	8±2.2*	0/10	NT
MSC + fMWCNT 1,000 ng/mL	5±1.8	0/10	NT
MSC + fCOx 10 ng/mL	2±1	0/10	NT
MSC + fCOx 100 ng/mL	2±1.1	0/10	NT
MSC + fCOx 1,000 ng/mL	2±0.75	0/10	NT

Notes: MSCs were treated for 7 days with different fCNT concentrations and, then, seeded in soft agar. The cell growth independence of anchorage is evaluated estimating the percentages of colony formation for each cellular group. No significant difference was found among treated MSC groups; perhaps with the exception of cells treated with 100 ng/mL of fMWCNTs, which remains still but rather far from the positive control values. fCNT-treated MSCs do not produce tumors when were subcutaneously injected in mice by groups of 10 individuals. After 30 days of the injection, mice were sacrificed and only mice injected with positive control B16F-10 cells produced tumors. Tumor size was calculated as volume (cm^3). Values are shown as mean ± standard deviation. *$P<0.05$.

Abbreviations: fCOxs, functionalized oxygen-doped multiwalled carbon nanotubes; fMWCNTs, functionalized multiwalled carbon nanotubes; MSCs, mesenchymal stem cells; NT, no tumor.

this malformation prevents completely the development of interventricular septum and consequently the individuality of the ventricular chambers. Therefore, these cardiac alterations are incompatible with normal chicken development.

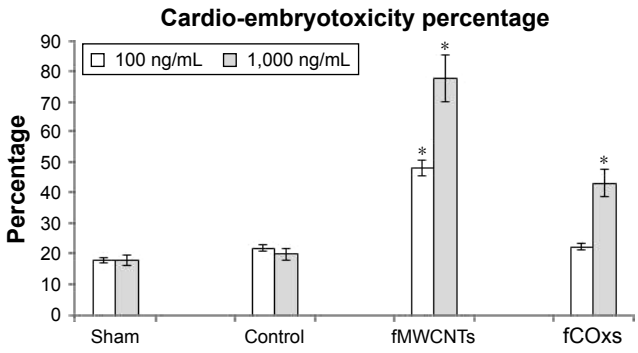

Figure 7 Cardiotoxic effect on chick embryos by CNTs.

Notes: fMWCNT and fCOx solutions (1.5 µL) were directly administered into pericardial cavity of chick embryos at stage HH 22 with 100 or 1,000 ng/mL and monitored during 1 week of treatment. Mortality rates were analyzed for each group with a remarkable increase both in fMWCNT solution and in the 1,000 ng/mL fCOx one. Values are shown as mean ± standard deviation (*$P<0.05$).

Abbreviations: CNTs, carbon nanotubes; fCOxs, functionalized oxygen-doped multiwalled CNTs; fMWCNTs, functionalized multiwalled CNTs; HH, Hamburger and Hamilton.

Interestingly, the embryos injected with fCOx did not produce morphological alterations and did not show any significant changes at 100 ng/mL; however, mortality increases by ~40% at the highest tested concentration (1,000 ng/mL).

Although also some types of morphological alterations considered as teratogenic are induced by fCNTs, such as anophthalmia, microphthalmia, and alterations in foot development, these are not significant. Analysis by confocal microscopy on sagittal sections of affected hearts shows (Figure 8B–F) nuclear colocalization of fMWCNT fragments into cardiomyocyte cell detected by the presence of myosin protein (shown in red in Figure 8E) but not in hearts injected with fCOx. The presence of cellular fragments, areas of fibrosis, and loss of cell junctions are also evident.

Discussion

At the concentrations of 10, 100, and 1,000 ng/mL, both fMWCNTs and fCOxs used in this study have a similar behavior, inducing cell proliferation once added to the MSC cultures. Our results agree with those reports indicating that the proliferation of different cell types is dose dependent according to the CNT concentrations.[3,54] Mooney et al[3] found that MSCs treated with CNTs for 6 days proliferate more than the control, which could be interpreted as a result of better adhesion among the CNT, the cells, and the contact surface and perhaps a kind of proliferation stimulation by the nanotubes.[55] This concern cannot be dismissed because it is known that CNT-treated cells are affected during the cell cycle and tend to increase the proliferation.[55–58]

We also found cell cycle alterations with shorter doubling times in fCNT-treated cells, which suggest a faster growth and consequently a greater proliferative process, instead a cell cycle blockage at followed by apoptosis, as is suggested by Rodriguez-Fernandez et al.[59]

These data could indicate that fCNTs would have a typical inductor factor behavior that could lead the MSCs toward a neoplastic state. In our own work, we have observed that the cells treated only with fMWCNTs can cause cell morphology alterations and probably nuclear damage, acquiring a shape that is notably similar to cells reported by Magrez et al[60] for lung cancer but rather absent in cells treated with fCOx. Ponti et al[61] have shown that, within a colony-forming efficiency assay, MWCNTs are able to interact with different cellular lines not inducing strong cytotoxic effect at the concentrations of 1–100 mg/mL.

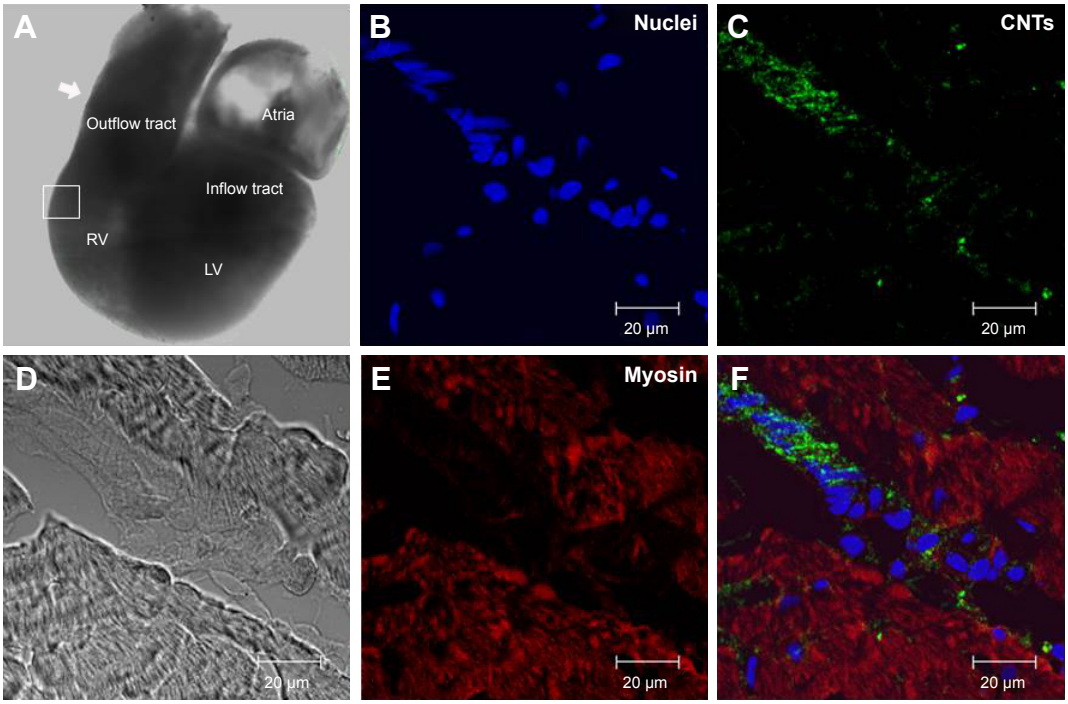

Figure 8 Cell damage on cardiomyocytes of chicken embryos.
Notes: fMWCNTs induce severe cardiac alterations. (**A**) Representative confocal images at 20× from whole embryo heart injected with fMWCNTs; the image shows an abnormal lateral position of the outflow tract (arrow) due to the loss of rotation of the heart. This malformation prevents the formation of the four cavities of the heart. The white square in (**A**) is amplified in (**B**–**F**) at 40×. (**B**) Cells' nucleus appears in blue. (**C**) fMWCNTs appear in green. (**D**) Transmission image appears in gray. (**E**) The myosin protein detected on cardiomyocytes is shown in red. (**F**) Nuclear colocalization of fMWCNTs inside cardiomyocytes. Scale bar =20 μm.
Abbreviation: CNTs, carbon nanotubes; fMWCNTs, functionalized multiwalled CNTs; LV, left ventricle; RV, right ventricle.

We were able to determinate the ability of a single cell to form a colony in soft agar using a clonogenic assay. Despite the morphological changes that were evidently induced by fMWCNTs, the appearance of colonies was notably low, but we persisted, and these clones were subcutaneously injected into nude mice where not a single clone could generate any type of tumor. Therefore, we did not find the direct correlation expected between colony forming and tumor growing in in vivo model. We know that in principle, MSCs have an unaltered genome. In an imperturbable genetic background, such as that of MSCs seems to have, all DNA repair systems are likely to be working well, which will result in an insufficient degree of aberrant morphology induced by contact with fCNTs, and an additional trigger may be required to induce a mutation that is essential for cell transformation in a neoplastic model. Another possible explanation is that the nanotubes interact with the actin skeleton, generating changes in the cell morphology and not necessarily cell transformation, but more studies are needed to explore this possibility. Longer period experiments would have to be done, during which all cells were always in contact with the fCNTs, to determine if this condition is sufficient for an eventual cell transformation.

Here, the chicken embryo model was used in an effort to understand if fCNTs could cause some risk or cell damage to the heart, thinking that in a near future, fCNTs could be used as essential elements for cardiac tissue scaffold designs. In addition to results previously reported in the chicken model, which suggest that CNTs can act as embryotoxic agent,[19] our results show evidence of causing a direct damage into cardiomyocytes by the uptake of fMWCNTs during cardiac tissue development. However, the heart or embryonic damages are not entirely evident when fCOxs were injected at concentrations below 1,000 ng/mL. Unlike fMWCNTs that can have severe biological effects both in treated cells in vitro or in cardiac cells directly injected into the hearts, fMWCNTs are highly cardioembryotoxic, raising the possibility of teratogenicity by the morphological anomalies found during embryological development.

Conclusion

Cell proliferation, cell cycle alteration, and drastic morphological changes increase when rat MSCs are treated with fMWCNTs.

However, these phenomena seem not to be enough because the MSCs seem not to modify their ability to

grow with anchorage independence, nor can they generate tumors or conduce cells to a neoplastic transformation process.

Our in vivo cytotoxicity results suggest that the exposure to fMWCNTs is highly cardioembryotoxic in comparison with fCOxs at 100 ng/mL, but the findings do not confirm if exposure to fCOx could influence chicken embryonic development in a dose-dependent manner. In both models, further studies are needed to fully understand the mechanism by which fCNTs can induce embryotoxicity or alterations. Oxidative stress is one probable cause, as suggested.[19] But also their uptake effect must be considered, which in last instance could depend on fCNTs' structural modifications and chemical reactivity as our experiments suggest. While it is true that cytotoxic effects at the cellular level are important and generate considerable controversy, more research is clearly needed to gain insight into the mechanism of these adverse effects, as well as the best ways to use CNTs and other nanomaterials without threatening the health of those who are exposed to them.

Acknowledgments

We wish to thank Gerardo Arrellín-Rosas and Raul Basilio Lara for their technical assistance. This study was supported by CONACYT-Project 101596 and Children's Hospital of Mexico Federico Gomez as a part of HIM/2015/021 SSA1166 Federal Grant. FCS acknowledges funding from the Department of Physics and Mathematics and the Research Division within UIA and the technical support of Samuel Rosas-Melendez, Mónica Ballesteros-Villareal, and Agustín Iñiguez-Rábago.

Disclosure

The authors report no conflicts of interest in this work.

References

1. Encabo-Berzosa MM, Sancho-Albero M, Crespo A, et al. The effect of PEGylated hollow gold nanoparticles on stem cell migration: potential application in tissue regeneration. *Nanoscale*. 2017;9(28):9848–9858.
2. Harrison BS, Atala A. Carbon nanotube applications for tissue engineering. *Biomaterials*. 2007;28(2):344–353.
3. Mooney E, Dockery P, Greiser U, Murphy M, Barron V. Carbon nanotubes and mesenchymal stem cells: biocompatibility, proliferation and differentiation. *Nano Lett*. 2008;8(8):2137–2143.
4. Yi C, Liu D, Fong C-C, Zhang J, Yang M. Gold nanoparticles promote osteogenic differentiation of mesenchymal stem cells through p38 MAPK pathway. *ACS Nano*. 2010;4(11):6439–6448.
5. Kroustalli AA, Kourkouli SN, Deligianni DD. Cellular function and adhesion mechanisms of human bone marrow mesenchymal stem cells on multi-walled carbon nanotubes. *Ann Biomed Eng*. 2013;41(12):2655–2665.
6. Correa-Duarte MA, Wagner N, Rojas-Chapana J, Morsczeck C, Thie M, Giersig M. Fabrication and biocompatibility of carbon nanotube-based 3D networks as scaffolds for cell seeding and growth. *Nano Lett*. 2004;4(11):2233–2236.
7. Nayak TR, Jian L, Phua LC, Ho HK, Ren Y, Pastorin G. Thin films of functionalized multiwalled carbon nanotubes as suitable scaffold materials for stem cells proliferation and bone formation. *ACS Nano*. 2010;4(12):7717–7725.
8. Kayat J, Gajbhiye V, Tekade RK, Jain NK. Pulmonary toxicity of carbon nanotubes: a systematic report. *Nanomedicine*. 2011;7(1):40–49.
9. Wick P, Manser P, Limbach LK, et al. The degree and kind of agglomeration affect carbon nanotube cytotoxicity. *Toxicol Lett*. 2007;168(2):121–131.
10. Zhu Y, Ran T, Li Y, Guo J, Li W. Dependence of the cytotoxicity of multi-walled carbon nanotubes on the culture medium. *Nanotechnology*. 2006;17(18):4668–4674.
11. Lam C-W, James JT, McCluskey R, Arepalli S, Hunter RL. A review of carbon nanotube toxicity and assessment of potential occupational and environmental health risks. *Crit Rev Toxicol*. 2006;36(3):189–217.
12. Nagai H, Toyokuni S. Biopersistent fiber-induced inflammation and carcinogenesis: lessons learned from asbestos toward safety of fibrous nanomaterials. *Arch Biochem Biophys*. 2010;502(1):1–7.
13. Sakamoto Y, Nakae D, Fukumori N, et al. Induction of mesothelioma by a single intrascrotal administration of multi-wall carbon nanotube in intact male Fischer 344 rats. *J Toxicol Sci*. 2009;34(1):65–76.
14. Takagi A, Hirose A, Nishimura T, et al. Induction of mesothelioma in p53± mouse by intraperitoneal application of multi-wall carbon nanotube. *J Toxicol Sci*. 2008;33(1):105–116.
15. Grosse Y, Loomis D, Guyton KZ, et al. Carcinogenicity of fluoro-edenite, silicon carbide fibres and whiskers, and carbon nanotubes. *Lancet Oncol*. 2014;15:1427–1428.
16. Cheng J, Flahaut E, Cheng SH. Effect of carbon nanotubes on developing zebrafish (*Danio rerio*) embryos. *Environ Toxicol Chem*. 2007;26(4):708–716.
17. Cheng J, Chan CM, Veca LM, et al. Acute and long-term effects after single loading of functionalized multi-walled carbon nanotubes into zebrafish (*Danio rerio*). *Toxicol Appl Pharmacol*. 2009;235(2):216–225.
18. Asharani PV, Lian Wu Y, Gong Z, Valiyaveettil S. Toxicity of silver nanoparticles in zebrafish models. *Nanotechnology*. 2008;19(25):255102.
19. Pietroiusti A, Massimiani M, Fenoglio I, et al. Low doses of pristine and oxidized single-wall carbon nanotubes affect mammalian embryonic development. *ACS Nano*. 2011;5(6):4624–4633.
20. Lim J-H, Kim S-H, Shin I-S, et al. Maternal exposure to multi-wall carbon nanotubes does not induce embryo-fetal developmental toxicity in rats. *Birth Defects Res B Dev Reprod Toxicol*. 2011;92(1):69–76.
21. Roman D, Yasmeen A, Mireuta M, Stiharu I, Al Moustafa AE. Significant toxic role for single-walled carbon nanotubes during normal embryogenesis. *Nanomedicine*. 2013;9(7):945–950.
22. Meng H, Xia T, George S, Nel AE. A predictive toxicological paradigm for the safety assessment of nanomaterials. *ACS Nano*. 2009;3(7):1620–1627.
23. Boehm HP. Surface oxides on carbon and their analysis: a critical assessment. *Carbon N Y*. 2002;40(2):145–149.
24. Gutiérrez-Praena D, Pichardo S, Sánchez E, Grilo A, Cameán AM, Jos A. Influence of carboxylic acid functionalization on the cytotoxic effects induced by single wall carbon nanotubes on human endothelial cells (HUVEC). *Toxicol In Vitro*. 2011;25:1883–1888.
25. Castle AB, Gracia-Espino E, Nieto-Delgado C, Terrones H, Terrones M, Hussain S. Hydroxyl-functionalized and N-doped multiwalled carbon nanotubes decorated with silver nanoparticles preserve cellular function. *ACS Nano*. 2011;5(4):2458–2466.
26. Singh A, Singh A, Sen D. Mesenchymal stem cells in cardiac regeneration: a detailed progress report of the last 6 years (2010-2015). *Stem Cell Res Ther*. 2016;7(1):82.

27. Hodgkinson CP, Gomez JA, Mirotsou M, Dzau VJ. Genetic engineering of mesenchymal stem cells and its application in human disease therapy. *Hum Gene Ther*. 2010;21:1513–1526.
28. Tandon V, Zhang B, Radisic M, Murthy SK. Generation of tissue constructs for cardiovascular regenerative medicine: from cell procurement to scaffold design. *Biotechnol Adv*. 2013;31(5):722–735.
29. Lee J, Abdeen AA, Zhang D, Kilian KA. Directing stem cell fate on hydrogel substrates by controlling cell geometry, matrix mechanics and adhesion ligand composition. *Biomaterials*. 2013;34(33):8140–8148.
30. Kharaziha M, Shin SR, Nikkhah M, et al. Tough and flexible CNT-polymeric hybrid scaffolds for engineering cardiac constructs. *Biomaterials*. 2014;35(26):7346–7354.
31. Zhou J, Chen J, Sun H, et al. Engineering the heart: evaluation of conductive nanomaterials for improving implant integration and cardiac function. *Sci Rep*. 2014;4(3733):1–11.
32. Miyagawa S, Sawa Y, Sakakida S, et al. Tissue cardiomyoplasty using bioengineered contractile cardiomyocyte sheets to repair damaged myocardium: their integration with recipient myocardium. *Transplantation*. 2005;80(11):1586–1595.
33. Bot PT, Hoefer IE, Piek JJ, Pasterkamp G. Hyaluronic acid: targeting immune modulatory components of the extracellular matrix in atherosclerosis. *Curr Med Chem*. 2008;15(8):786–791.
34. Tsimbouri P, Gadegaard N, Burgess K, et al. Nanotopographical effects on mesenchymal stem cell morphology and phenotype. *J Cell Biochem*. 2014;115(2):380–390.
35. Khetan S, Guvendiren M, Legant WR, Cohen DM, Chen CS, Burdick JA. Degradation-mediated cellular traction directs stem cell fate in covalently crosslinked three-dimensional hydrogels. *Nat Mater*. 2013;12(5):458–465.
36. Murphy WL, McDevitt TC, Engler AJ. Materials as stem cell regulators. *Nat Mater*. 2014;13(6):547–557.
37. Pantel K, Alix-Panabières C. Bone marrow as a reservoir for disseminated tumor cells: a special source for liquid biopsy in cancer patients. *Bonekey Rep*. 2014;3:584.
38. Terrones M, Filho AS, Rao A. Doped carbon nanotubes: synthesis, characterization and applications. *Carbon Nanotubes*. 2008;566:531–566.
39. Botello-Méndez A, Campos-Delgado J, Morelos-Gómez A, et al. Controlling the dimensions, reactivity and crystallinity of multiwalled carbon nanotubes using low ethanol concentrations. *Chem Phys Lett*. 2008;453(1–3):55–61.
40. Shabestari ME, Kalali EN, González VJ, et al. Effect of Nitrogen and Oxygen Doped Carbon Nanotubes on Flammability of Epoxy Nanocomposites. *Carbon*. 2017;121:193–200.
41. Botello-Méndez AR, López-Urías F, Terrones M, Terrones H. Magnetic behavior in zinc oxide zigzag nanoribbons. *Nano Lett*. 2008;8(6):1562–1565.
42. Andrews R, Jacques D, Rao AM, et al. Continuous production of aligned carbon nanotubes: a step closer to commercial realization. *Chem Phys Lett*. 1999;303(5–6):467–474.
43. Liu J, Rinzler AG, Dai H, et al. Fullerene pipes. *Science*. 1998;280(5367):1253–1256.
44. Liu D, Yi C, Zhang D, Zhang J, Yang M. Inhibition of proliferation and differentiation of mesenchymal stem cells by carboxylated carbon nanotubes. *ACS Nano*. 2010;4(4):2185–2195.
45. Nunez R. DNA measurement and cell cycle analysis by flow cytometry. *Curr Issues Mol Biol*. 2001;3(3):67–70.
46. Hayflick L. *Tissue Culture Methods and Applications*. New York: Academic Press; 1973:220.
47. Minati L, Speranza G, Bernagozzi I, et al. Investigation on the electronic and optical properties of short oxidized multiwalled carbon nanotubes. *J Phys Chem C*. 2010;114(25):11068–11073.
48. Shin SI, Freedman VH, Risser R, Pollack R. Tumorigenicity of virus-transformed cells in nude mice is correlated specifically with anchorage independent growth in vitro. *Proc Natl Acad Sci U S A*. 1975;72(11):4435–4439.
49. Pantelouris EM. Observations on the immunobiology of 'nude' mice. *Immunology*. 1971;20:247–252.
50. Bullard DE, Schold SC Jr, Bigner SH, Bigner DD. Growth and chemotherapeutic response in athymic mice of tumors arising from human glioma-derived cell lines. *J Neuropathol Exp Neurol*. 1981;40(4):410–427.
51. Hamburger V, Hamilton HL. A series of normal stages in the development of the chick embryo. *Dev Dyn*. 1951;88(1):49–92.
52. González VJ, Martín-Alberca C, Montalvo G, et al. Carbon nanotube-Cu hybrids enhanced catalytic activity in aqueous media. *Carbon N Y*. 2014;78:10–18.
53. Schneider CA, Rasband WS, Eliceiri KW. NIH Image to ImageJ: 25 years of image analysis. *Nat Methods*. 2012;9(7):671–675.
54. De Nicola M, Nuccitelli S, Gattia DM, et al. Effects of carbon nanotubes on human monocytes. *Ann N Y Acad Sci*. 2009;1171:600–605.
55. Di Sotto A, Chiaretti M, Carru GA, Bellucci S, Mazzanti G. Multiwalled carbon nanotubes: lack of mutagenic activity in the bacterial reverse mutation assay. *Toxicol Lett*. 2009;184(3):192–197.
56. Holy J, Perkins E, Yu X. Adhesion, proliferation and differentiation of pluripotent stem cells on multi-walled carbon nanotubes. *IET Nanobiotechnol*. 2011;5(2):41–46.
57. Woo KM, Chen VJ, Ma PX. Nano-fibrous scaffolding architecture selectively enhances protein adsorption contributing to cell attachment. *J Biomed Mater Res A*. 2003;67:531–537.
58. Zhu L, Chang DW, Dai L, Hong Y. DNA damage induced by multiwalled carbon nanotubes in mouse embryonic stem cells. *Nano Lett*. 2007;7(12):3592–3597.
59. Rodriguez-Fernandez L, Valiente R, Gonzalez J, Villegas JC, Fanarraga ML. Multiwalled carbon nanotubes display microtubule biomimetic properties in vivo, enhancing microtubule assembly and stabilization. *ACS Nano*. 2012;6(8):6614–6625.
60. Magrez A, Kasas S, Salicio V, et al. Cellular toxicity of carbon-based nanomaterials. *Nano Lett*. 2006;6(6):1121–1125.
61. Ponti J, Colognato R, Rauscher H, et al. Colony forming efficiency and microscopy analysis of multi-wall carbon nanotubes cell interaction. *Toxicol Lett*. 2010;197(1):29–37.